

Electronic supplementary information

Fluoride-bridged {Ln₂Cr₂} polynuclear complexes from semi-labile *mer*-[CrF₃(py)₃] and [Ln(hfac)₃(H₂O)₂]

Christian Aa. Thuesen,^a Kasper S. Pedersen,^a Magnus Schau-Magnussen,^a Marco Evangelisti,^b Høgni Weihe,^a Stergios Piligkos,^a Johan Vibenholt,^a and Jesper Bendix^{a*}

1 Crystallographic data

Table S1. Single-crystal data and structure refinement details. Note that **1Ln** ($\text{Ln} = \text{Y}$ (powder), Tb , Ho , Er) are isomorphous to **1Dy**, see Fig. S1a below.

	1Y	1Gd	1Dy	2Tb	3Dy
Formula	$\text{C}_{50}\text{H}_{28}\text{Cr}_2\text{F}_{40}\text{N}_4\text{O}_{14}\text{Y}_2$	$\text{C}_{50}\text{H}_{28}\text{Cr}_2\text{F}_{40}\text{Gd}_2\text{N}_4\text{O}_{14}$	$\text{C}_{50}\text{H}_{28}\text{Cr}_2\text{Dy}_2\text{F}_{40}\text{N}_4\text{O}_{14}$	$\text{C}_{60}\text{H}_{36}\text{Cr}_2\text{F}_{42}\text{N}_6\text{O}_{12}\text{Tb}_2$	$\text{C}_{35}\text{H}_{21}\text{CrDyF}_{26}\text{N}_3\text{O}_9 \cdot 0.82(\text{CH}_2\text{Cl}_2)$
M_r	1950.58	2087.26	2097.76	2252.79	1406.11
Crystal size/mm	$0.20 \times 0.08 \times 0.03$	$0.18 \times 0.09 \times 0.07$	$0.12 \times 0.07 \times 0.06$	$0.37 \times 0.13 \times 0.13$	$0.23 \times 0.12 \times 0.09$
Shape	Plate	Prism	Prism	Rod	Prism
Colour	Pink	Pink	Pink	pink	Pink
Crystal system	Triclinic	Triclinic	Triclinic	Triclinic	Triclinic
Space group	$P\bar{1}$	$P\bar{1}$	$P\bar{1}$	$P\bar{1}$	$P\bar{1}$
T/K	122	122	122	122	122
$a/\text{\AA}$	12.181(2)	12.158(3)	11.115(4)	12.5395(9)	12.404(3)
$b/\text{\AA}$	12.530(3)	12.5405(14)	12.695(3)	13.2423(10)	20.093(3)
$c/\text{\AA}$	12.550(2)	12.5573(10)	12.939(3)	15.094(2)	20.130(2)
α°	65.253(11)	65.482(10)	95.30(2)	97.193(16)	88.972(9)
β°	78.007(12)	78.496(14)	99.06(3)	110.446(8)	85.810(11)
γ°	77.683(13)	77.792(12)	101.86(2)	116.354(7)	83.452(11)
$V/\text{\AA}^3$	1684.4(6)	1689.1(5)	1749.7(7)	1983.6(3)	4970.7(14)
Z	1	1	1	1	4
$\rho/\text{g cm}^{-3}$	1.923	2.052	1.991	1.886	1.879
$\mu(\text{Mo K}\alpha)/\text{mm}^{-1}$	2.19	2.42	2.58	2.19	1.95
$2\theta_{\max}/^{\circ}$	28.1	40.0	27.7	40.0	27.7
$F(000)$	954	1004	1008	1090	2731
Reflections collected	63568	90679	63297	130374	184854
Unique reflections	8156	20879	8083	24542	22902
R_{int}	0.060	0.094	0.097	0.056	0.105
Refl. Observed [$I > 2\sigma(I)$]	6691	16431	6597	20391	16551
Parameters/restraints	508/1	508/1	508/1	559/0	1417/4
GOF on F^2	1.07	1.09	1.06	1.06	1.14
$R[F^2 > 2\sigma(F^2)]$	0.043	0.042	0.046	0.030	0.052
wR ₂ (all data)	0.096	0.103	0.108	0.071	0.120
Largest residuals/e \AA^{-3}	1.24/−0.90	1.52/−1.59	1.79/−1.49	2.13/−0.90	1.39/−0.94

2 Powder diffractograms

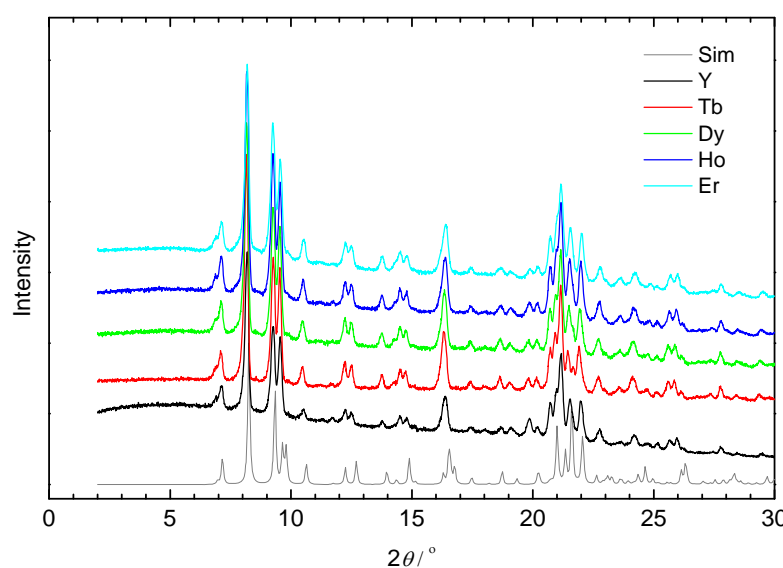


Fig. S1a. Powder diffractograms of the **1Ln** series. The grey diffractogram is calculated from the crystal structure of **1Dy**.

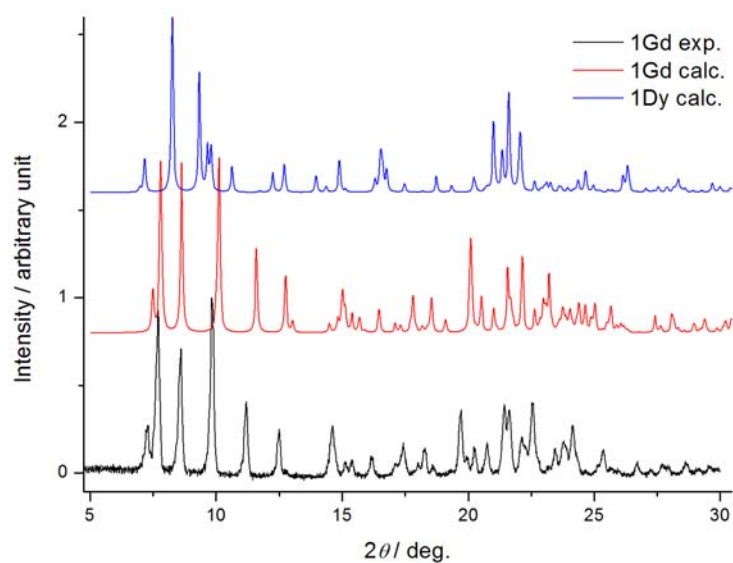


Fig. S1b. Powder diffractogram of **1Gd**. The different nature of **1Gd** as compared to **1Dy** (**1Ln**) illustrated by experimental and calculated powder diffractograms.

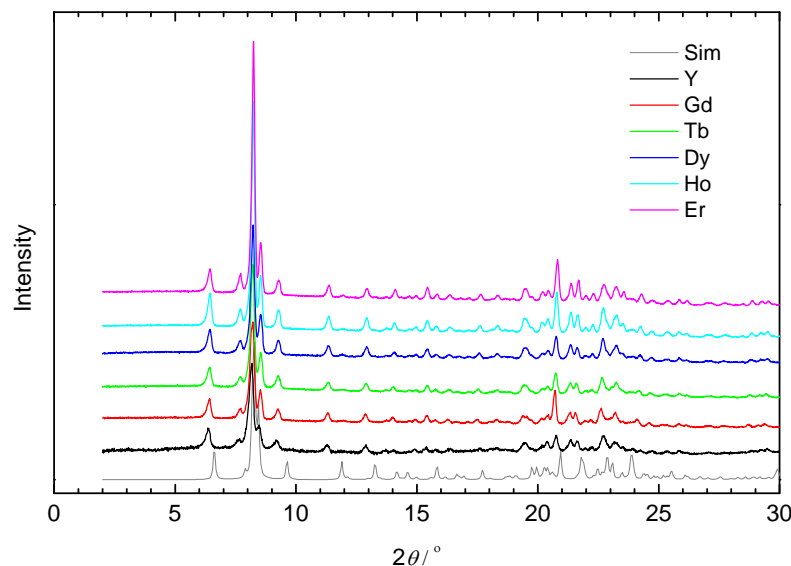
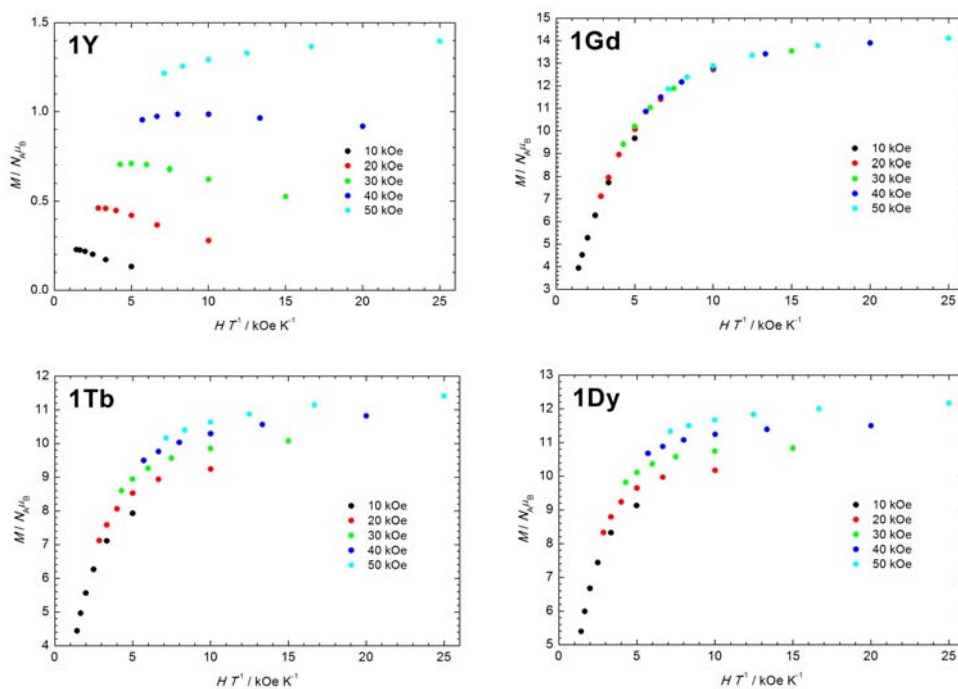


Fig. S2. Powder diffractograms of the **2Ln** series. The grey diffractogram is calculated from the crystal structure of **2Dy**.

3 Magnetic data



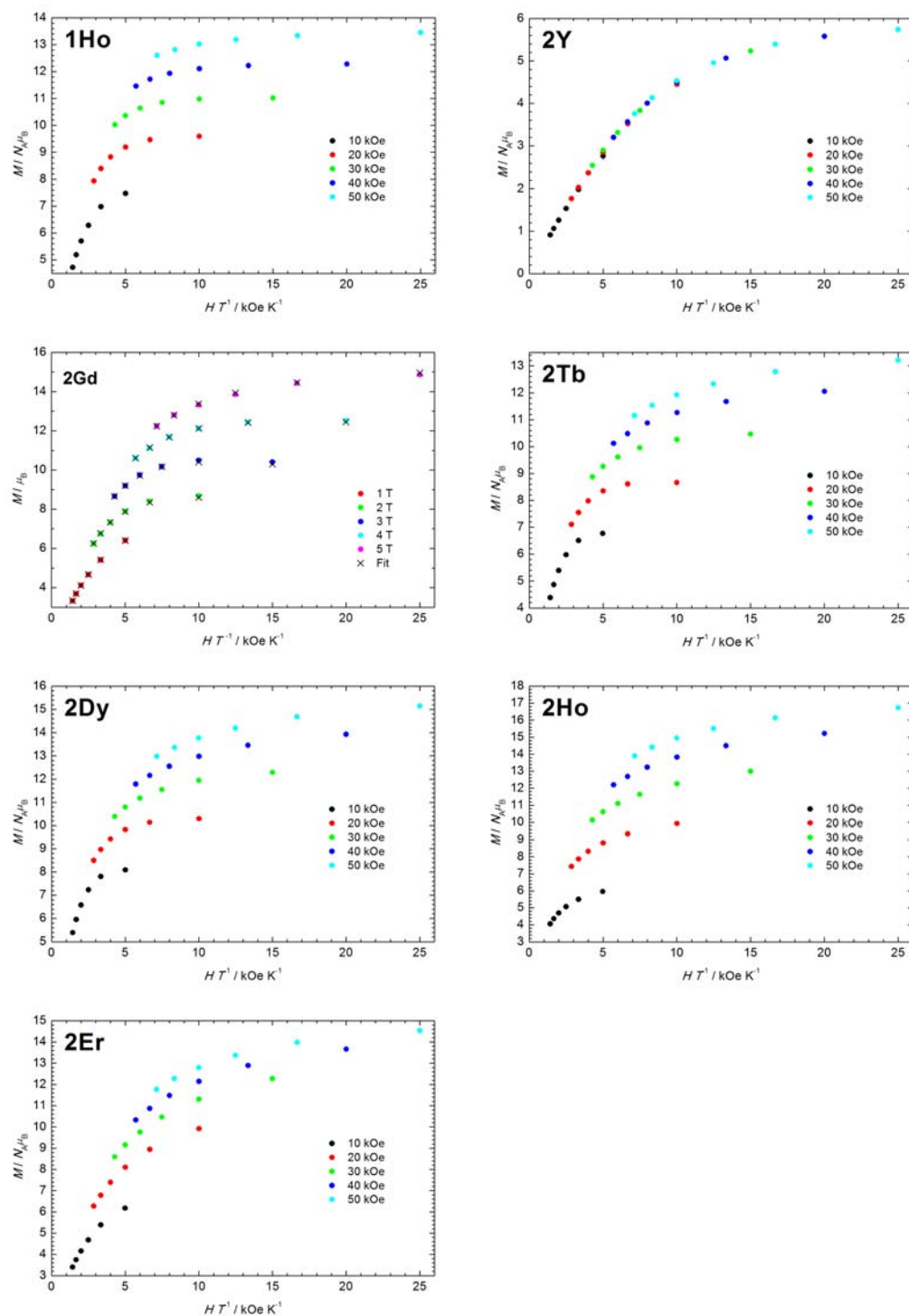


Fig. S5. Magnetization data.

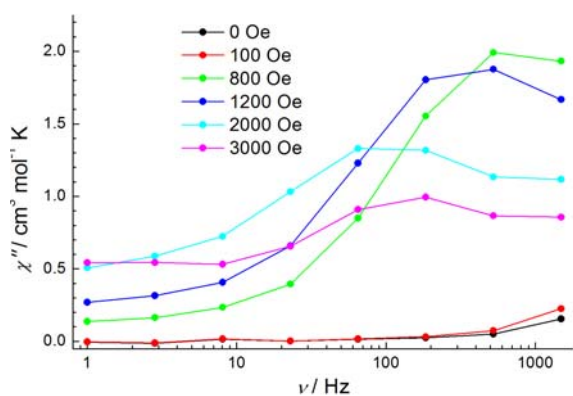


Fig. S6. Field dependence of the out-of-phase component of the ac susceptibility of **1Dy** at $T = 1.8 \text{ K}$

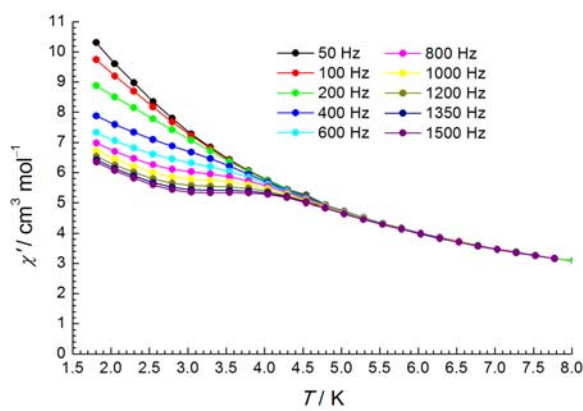


Fig. S7. In-phase component of the ac susceptibility of **1Dy** obtained with $H_{\text{dc}} = 1200 \text{ Oe}$.

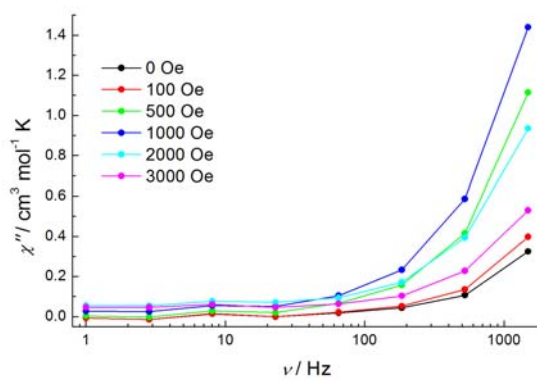


Fig. S8. Field dependence of the out-of-phase component of the ac susceptibility of **2Dy** at $T = 1.8 \text{ K}$

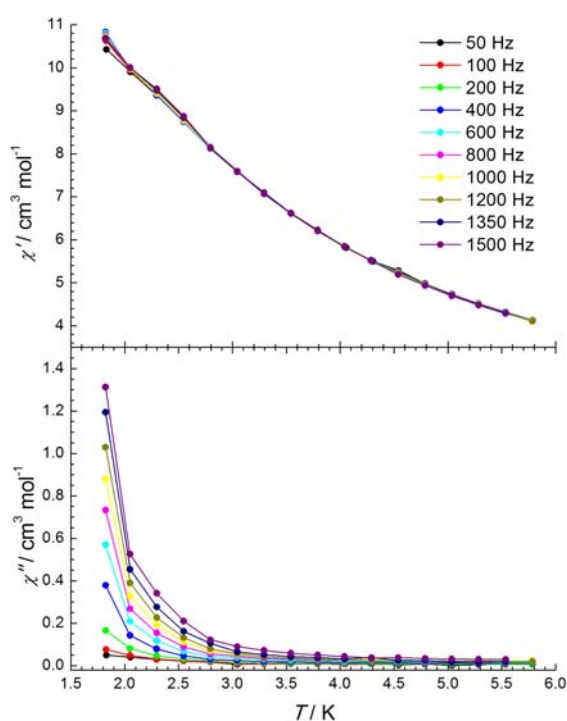


Fig. S9. Out-of-phase (top) and in-phase (bottom) component of the ac susceptibility of **2Dy** obtained with $H_{\text{dc}} = 1200$ Oe.

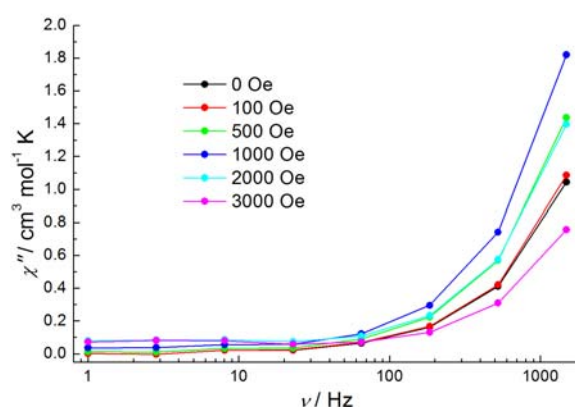


Fig. S10. Field dependence of the out-of-phase component of the ac susceptibility of **2Tb** at $T = 1.8$ K